J. Membrane Biol. 84, 9–23 (1985)

The Journal of
Membrane Biology

Experimental and Theoretical Studies on Tl^+ Interactions with the Cation-Selective Channel of the Sarcoplasmic Reticulum

James Fox* and Sergio Ciani
Brain Research Institute (Ahmanson Laboratory of Neurobiology), Department of Physiology, and Jerry Lewis Neuromuscular Research Center, University of California at Los Angeles, Los Angeles, California 90024

Summary. This paper presents an experimental study and a theoretical interpretation of the effects of thallous ion on the electrical properties of the cation-selective channel of the sarcoplasmic reticulum (SR channel). The properties of this channel in solutions which do not contain thallous ion are consistent with the predictions of Läuger's theory for singly occupied pores (P. Läuger, 1973, *Biochim. Biophys. Acta* **311**:423–441). However, this theory does not account for SR channel properties in mixtures containing thallous ion. SR channel conductance is less than predicted in mixed salt solutions of thallium with either potassium or ammonium (J. Fox, 1983, *Biochim. Biophys. Acta* **736**:241–245), yet is greater than expected in mixtures of lithium and thallium. In a simple single-ion pore, the ratio of the products of the single-salt binding constants and maximum conductances is equal to the permeability ratio calculated from zero-current potential experiments under near equilibrium conditions. This is not found for the SR channel when thallous ion is present. SR channel properties in the presence of thallous ion can, however, be explained by a model which postulates the existence of two external modulatory sites on the channel, without implying double-occupancy in the permeation pathway. When thallous ion is bound to a modulatory site the maximum conductance of the channel to all permeating ions is altered (thallous included). Two other models (a three-barrier, two-internal-site pore which allows multiple occupancy, and a pore with fluctuating barriers) are discussed, but are found to be unable to fit our conductance data at different concentrations.

Key Words thallium · SR cation channel · channel model

Introduction

This paper describes thallous ion permeation in the cation-selective channel of rabbit sarcoplasmic reticulum (SR channel). Previous work (Fox, 1983; 1984) has shown that this channel is permeant to thallous ion, and that channel conductance in mixed cation solutions containing thallous ion is less than expected by simple one-ion pore models. In this paper we present a more extensive description of these effects, including the new finding that the thallous ion can enhance the conductance of the SR channel in mixtures with lithium, and we also propose a model to account for all of these effects.

The Cation-Selective Channel of the Sarcoplasmic Reticulum

The SR channel is a protein channel selective for monovalent cations, first described in artificial membranes by Miller and his coworkers (Miller & Racker, 1976; Miller, 1978; Miller & Rosenberg, 1979*a*,*b*; Coronado, Rosenberg & Miller, 1980; Labarca, Coronado & Miller, 1980). It can be inserted into artificial bilayer membranes, where its electrical properties can be examined under controlled conditions (Miller, 1978). When SR vesicles are presented to one membrane face only, virtually all of the inserted channels have the same orientation, as determined by the asymmetric response to applied voltage, blockers and proteolytic enzymes (Miller, 1978; Coronado & Miller, 1979; Miller & Rosenberg, 1979*a*,*b*; Labarca et al., 1980; Miller, 1982*b*).

The conductance of the open state in symmetric single-salt solutions saturates with increasing ion concentration, with a maximum limiting conductance in PE-PC bilayers of 223 pS for potassium and 7 pS for lithium (Bell & Miller, 1983). Zero-current potentials measured under bi-ionic conditions do not vary with the total ion concentration, and permeability ratios calculated from these potentials are equal to the conductance ratio for the same pair of ions at low concentration. These data are consistent with a simple single-ion pore model for the SR channel (Coronado et al., 1980).

Channel current increases nearly linearly with applied potential through the open channel for both

* *Present address:* Jules Stein Eye Institute, U.C.L.A.

positive and negative potentials (Coronado et al., 1980; Labarca et al., 1980). Current through the SR channel may be blocked in a voltage-dependent, competitive manner by various divalent cations (Miller, 1978), cesium (Coronado & Miller, 1979), several monovalent quaternary ammonium ions (Coronado & Miller, 1982) and several bis-quaternary ammonium compounds (Coronado & Miller, 1980; Miller, 1982*b*). The blocking data is consistent with a single-ion pore model of SR channel conductance (Coronado & Miller, 1982; Miller, 1982*b*).

In summary, the rabbit SR channel is permeant to monovalent cations, blocked in a voltage-dependent, competitive fashion by several organic cations and cesium, and behaves like a one-ion pore. More detailed information on the properties of this system may be found in recent reviews (Miller, 1982*a*; 1983).

Thallous Ion Effects on Cation Channels

The thallous ion exhibits anomalous behavior in many cation channels in that, while permeant, it blocks current when present in mixed-salt solutions. It is more permeant than potassium in the potassium channel of squid (Hagiwara et al., 1972), frog node of Ranvier (Hille, 1973), in the anomalous rectifier channel of starfish egg (Hagiwara et al., 1977) and frog muscle (Gay, 1981; Ashcroft & Stanfield, 1983), and as permeant in the gramicidin channel (Andersen, 1975; Eisenman, Sandblom & Neher, 1977). Yet, anomalous rectifier channel conductance goes through a minimum at low mole fractions of thallium in mixed thallium-potassium solutions in starfish egg (Hagiwara & Takahashi, 1974; Hagiwara et al., 1977) and frog muscle (Ashcroft & Stanfield, 1983). The same effect is seen with gramicidin channel conductance in mixtures of thallium with sodium (Neher, 1975) or potassium (Andersen, 1975).

Thallium effects in gramicidin have been modeled as being due simply to occupation of the channel by both thallium and potassium at one time (Urban, Hladky & Haydon, 1978; Hladky, Urban & Haydon, 1979), or to multiple occupancy in concert with ion binding to external modulatory sites (Eisenman et al., 1977; Sandblom, Eisenman & Neher, 1977).

Alternatively, the thallous ion effects observed in the anomalous rectifier channel have been accounted for by modifying a single-ion pore model for that channel (Ciani et al., 1978) by postulating that the conductance and gating properties of this channel are altered when thallous ions are bound to an external "gating site" (Krasne et al., 1983).

Thus, similar thallous ion effects have been accounted for by dissimilar models, some of which allow only one ion to occupy a pore at any one time, others allowing multiple occupancy of the pore. Although these two kinds of models can make similar quantitative predictions, we find that the one-ion model better fits our data.

Materials and Methods

Preparation of the Sarcoplasmic Reticulum Vesicles

Rabbit sarcoplasmic reticulum vesicles (SR vesicles) were prepared by the method of Miller and Rosenberg (1979*a*), and stored in 0.4 M sucrose in glass tubes at −70°C until use. The final concentration of the SR vesicle solution in sucrose was 4 to 8 mg protein per ml solution. Calcium uptake, measured with ^{45}Ca label as detected by liquid scintillation counter, was used to assay the condition of the vesicles. Typically, 100,000 cpm were observed for a 50-μl aliquot of the vesicle preparation (corresponding to roughly 300 nM Ca^{2+} taken up per mg protein per minute over 5 min).

Solutions

Acetate salts were used in all solutions to insure adequate thallium solubility. Salt solutions also contained 5 mM MOPS or HEPES buffer, and 0.1 mM EDTA, at pH 7.0 (set with Tris or KOH). Solutions were made fresh each day, either from the dry salts or from stock 1 M solutions. All solutions were filtered with a 0.22 μm pore diameter disposable filter just before use.

Activity coefficients are from the Tables in Robinson and Harned (1941). Coefficients for concentrations below 0.1 M were calculated by the method of Guggenheim as described in the above reference.

Bilayer Formation

Mueller-Rudin bilayers were formed from a 90% L-alpha-dioleoyl phosphatidyl ethanolamine (PE) and 10% L-alpha-dioleoyl phosphatidyl choline (PC) mixture in decane (10 mg lipid per ml decane), made fresh each day. Lipids were purchased from Avanti Polar Lipids, and the decane from Sigma Chemical Company. These bilayers were formed across a small (0.3 to 0.5 mm) hole in the wall of a polystyrene test tube held in a Plexiglas® chamber with an optically flat glass window. The bilayer separated the solution inside the test tube (the *trans* pool, containing approximately 3 ml) from the solution in the Plexiglas® chamber (the *cis* pool, approximately 7 ml). Although these membranes were generally quite stable, after fusion of the sarcoplasmic reticulum vesicles they became unstable at high voltages. Membrane instability increased as the concentration of thallium was increased both in single-salt and mixed solution experiments.

Montal-Mueller bilayers were formed across a hole (0.1 to 0.2 mm) melted into a piece of 13 μm thick Teflon sheet which covered a "V" cut in a septum separating two pools in a Teflon chamber. These membranes were made from mixtures of PE and PC or PE and PS, at a concentration of 10 mg/ml in pentane.

Channel Insertion into the Membrane

Once a membrane was formed and a stable baseline observed, SR vesicle solution was added to the *cis* pool in the presence of 1 mM calcium with stirring (to a final concentration of 50 to 100 μg of protein per milliliter), with the membrane potential held at +40 mV. In some cases with the Montal membranes, an osmotic gradient was created across the membrane by addition of sucrose to the *cis* pool to enhance channel insertion. Once channel steps were observed, the voltage was set to zero and EDTA was added in order to prevent further insertion.

Electronics

Single-channel current steps were monitored with a high-gain current-to-voltage converter, consisting either of a Function Module 380K amplifier with a 1 GΩ feedback resistor, or, of a circuit patterned after the patch clamp amplifier described in Hamill et al. (1981). Electrical connection to the bathing solutions was via Ag/AgCl electrodes and agar bridges, the *cis* pool being connected to the voltage source (a battery), and the *trans* pool to virtual ground.

Channel Conductance Measurements

The single-channel conductances reported in this paper are the average of the experimental conductances found at + and − 20 mV applied voltage (in some cases values from + and − 40 mV were included when the current was too small for reliable measurements at 20 mV). These conductance values are meant to approximate the zero-current conductance of the SR channel.

Results

The theory and experiments described in this section deal with the effects of thallium on the electrical properties of single SR channels in pure thallium acetate solutions, and in mixed solutions containing thallium and another permeant cation. Some of the data presented here have been reported previously (Fox, 1983; 1984), but are presented again in this paper to illustrate the fit of the model to the complete set of measurements.

Theoretical Results

The model which we developed is described in detail in Appendix A. In this section, we present only the main results which will be used to fit the experimental data. In agreement with Coronado et al. (1980), we postulate that the pore of the SR channel may be occupied by only a single ion, but we also make the further assumption that there are two external binding sites on the channel, one at each side, and that when a thallous ion is bound to one of them, the conductance properties of the channel are

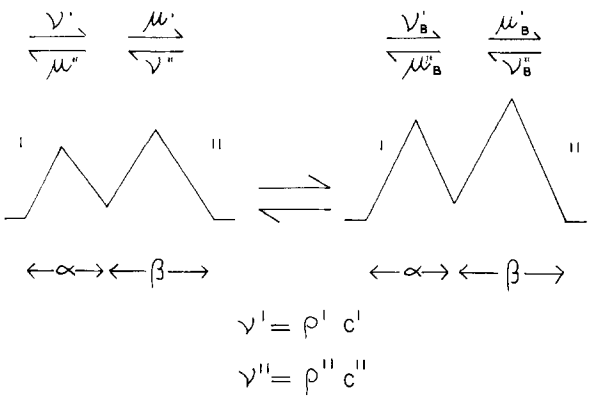

Fig. 1. This diagram illustrates our conception of the SR channel pore in terms of the energy barriers an ion would encounter during permeation. The pore may be found in either the "unbound" state, or, following thallous ion binding to one of the external modulatory sites, the "bound" state. The symbols above the arrows (which indicate the directions of ion flow) denote the ion jump rates. According to our assumptions, the transition of the pore between the "unbound" and the "bound" states does not alter the depth of the well, and leaves the relative heights of the barriers unchanged

altered. We assume that other cations may compete with thallous ion for binding to these external sites, but that only thallous ion binding alters the permeability properties. A diagram illustrating some features of the channel is shown in Fig. 1.

Applying Eyring rate theory to a two-barrier, one-internal-site pore model, the following equation which describes the zero-current conductance is obtained:

$$g_o = \frac{(1 + 2K_B C_T)^{-1}}{1 + K_K C_K + K_T C_T} \{g_K^{\max} K_K C_K + g_T^{\max} K_T C_T + 2K_B C_T [g_{BK}^{\max} K_K C_K + g_{BT}^{\max} K_T C_T]\} \quad (1)$$

for a membrane separating symmetrical solutions containing two permeant cations. In this, as well as the following equations, the subscript T represents thallium, and K the other cation. Thus, K may represent K^+, Na^+, NH_4^+, or Li^+. C_T and C_K are the ion concentrations, while K_K and K_T are the ion binding constants to the internal site of the channel (which, according to our model, are the same regardless of the occupancy state of the modulatory site). Thallous ion binding to the external sites is described by the effective binding constant K_B; $g_K^{\max}$ and $g_T^{\max}$ are the maximum channel conductances in single-salt solutions of the subscripted ion for a channel with no thallous ion bound to an external site, while $g_{BK}^{\max}$ and $g_{BT}^{\max}$ are the same quantities when a thallous ion is bound to one of the external sites. When expressed as functions of the rate constants of perme-

ation, defined in Fig. 1, the binding constants to the internal site and the maximum conductances are

$$K_i = \frac{\bar{\rho}_i'}{\bar{\mu}_i''} = \frac{\bar{\rho}_i''}{\bar{\mu}_i'} = \frac{\bar{\rho}_{Bi}'}{\bar{\mu}_{Bi}''} = \frac{\bar{\rho}_{Bi}''}{\bar{\mu}_{Bi}'} \; (i = K, T) \tag{2}$$

and

$$g_l^{\max} = \frac{e^2}{kT} \cdot \frac{\bar{\mu}_l' \bar{\mu}_l''}{\bar{\mu}_l' + \bar{\mu}_l''} \; (l = K, T, BK, BT). \tag{3}$$

Note that it is possible to describe the binding constants K_i in terms of the rate constants for both "bound" and "unbound" pores [as in Eq. (2)] as a consequence of an assumption of our model (assumption 6 in Appendix A) and of microscopic reversibility.

The parameter K_B, which has been introduced mainly to shorten the equations, could be called the effective binding constant of Tl^+ to the external modulatory sites and is defined, in terms of the real binding constants, K_{BT} and K_{BK}, by

$$K_B = \frac{K_{BT}}{1 + K_{BK}(C_K' + C_K'')}. \tag{4}$$

When the solutions are symmetrical, as in the case of Eq. (1), the denominator reduces to $1 + 2K_{BK}C_K$.

Single-Channel Conductance for Arbitrary Voltage

At voltages away from zero, the conductance in symmetric mixtures can be described by the following expression:

$$g(u) = \frac{e^u - 1}{u} \cdot \frac{P_K C_K + P_T C_T}{(1 + 2K_B C_T)\left(1 + \frac{\nu_K}{\mu_K} + \frac{\nu_T}{\mu_T}\right)} \tag{5}$$

where the parameters thus far undefined have the following meanings: u is the potential in units of kT/e, ν_K/μ_K and ν_T/μ_T are

$$\frac{\nu_i}{\mu_i} = \frac{\nu_i' + \nu_i''}{\mu_i' + \mu_i''} = K_i C_i \frac{1 + R_i e^{u/2}}{1 - 2\alpha + R_i e^{(1-2\alpha)u/2}} \; (i = K, T) \tag{6}$$

where K_i and α are defined in Eq. (2) and in Fig. 1, respectively, and

$$R_i = \frac{\bar{\mu}_i'}{\bar{\mu}_i''} \; (i = K, T). \tag{7}$$

Finally, the two quantities, P_K and P_T, are

$$P_i = e^{(\alpha - 1)u/2} K_i \frac{1 + R_i}{1 + R_i e^{u/2}} \{g_i^{\max} + 2K_B C_T g_{Bi}^{\max}\} \; (i = K, T) \tag{8}$$

where all the parameters on the right-hand side have been defined previously.

Zero-Current Potential

When the channel is in a membrane separating different ionic solutions, the expression for the zero-current potential can be cast in a form similar to the Goldman-Hodgkin-Katz equation, in which the permeability ratio is given by

$$\frac{P_K}{P_T} = \frac{K_K}{K_T} \frac{1 + R_K}{1 + R_T} \cdot \frac{1 + R_T e^{u/2}}{1 + R_K e^{u/2}} \cdot \frac{g_K^{\max} + K_B(C_T' + C_T'')g_{BK}^{\max}}{g_T^{\max} + K_B(C_T' + C_T'')g_{BT}^{\max}}. \tag{9}$$

The permeability ratio, P_T/P_K, becomes voltage independent when $R_K = R_T$, a requirement that coincides with the condition that the difference between the two energy peaks be the same for the two ions. Note also that if K_B is so large that

$$g_K^{\max} < K_B(C_T' + C_T'')g_{BK}^{\max} \tag{10}$$

for at least some experimental values of the thallium concentrations, the permeability ratio P_T/P_K is not relatable to the ratio of the zero-current conductances in single-salt solutions. This case applies to our system, since the fitting value of K_{BT} is indeed very high, and the conductance ratio for K^+ and Tl^+ does not agree with the permeability ratio.

Experimental Results

SR Channel Conductance in Thallium Acetate

Single-channel current steps were recorded in thallium acetate solutions at several concentrations. Current records from these single-salt experiments are shown in Fig. 2. A plot of channel conductance (as measured from current traces such as these) versus thallium concentration is shown in Fig. 3. SR channel conductance approaches a limiting value of 57.5 pS, with an apparent dissociation constant of 18.25 mM (corresponding to 54.8 M^{-1}). According to our model, these are the values of $g_{BT}^{\max}$ and K_T, respectively. (The observed maximum limiting conductance in pure thallium corresponds to $g_{BT}^{\max}$ and not $g_T^{\max}$ since, in our model, the external sites will saturate at high thallous ion concentration along with the internal site in the permeation pathway.)

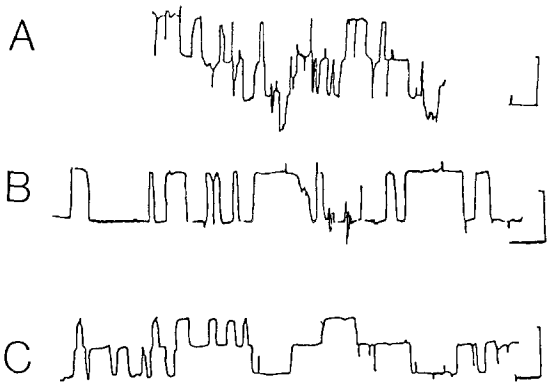

Fig. 2. SR channel current steps at three concentrations of symmetric thallium acetate. *A*. 0.05 M; *B*. 0.1 M; and *C*. 0.5 M (90% PE-10% PC membranes in decane). Horizontal bars: 15 sec; vertical bars: *A*, 50 pS; *B*, 50 pS; *C*, 100 pS

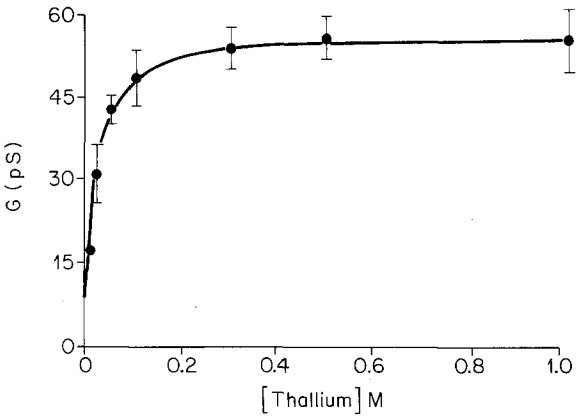

Fig. 3. SR channel conductance at various concentrations of symmetric thallium acetate solutions. Channels were incorporated into new 90% PE-10% PC decane-containing membranes for each experimental concentration. The points represent the averages of channel conductances found at ±20 mV (with ±40 mV included as well if currents were too small at ±20). The curve is drawn according to our model. These data are also fit by the equation derived by Läuger (1973) for the conductance of a single-ion channel as a function of concentration with a g^{max} of 57.5 pS and a K_T of 54.8 M^{-1}

These data are shown with the curve generated by Eq. (1) for the case of $C_K = 0$.

The g_{BT}^{max} for thallous ion is well below that of potassium in this channel, and is close to the 77 pS value for sodium, while the thallium binding constant K_T is near to the 52.6 M^{-1} reported for lithium (Coronado et al., 1980).

Mole Fraction Experiments

The SR channel has been characterized as a single-ion channel (Coronado et al., 1980). Accordingly, the one-ion pore theory of Läuger should account for the conductance observed when the SR channel is in a membrane which separates symmetric solutions containing two permeant ion species (Läuger, 1973). This theory adequately describes SR channel conductance for mixed potassium and sodium solutions, as is illustrated by the theoretical curve in Fig. 4. The total cation concentration was 0.1 M in each solution used in this series of experiments, while the mole fraction of each ion varied from 0 to 100% (mole fraction is defined as the concentration of one of the cations divided by the total cation concentration in the mixture). Only g^{max} and K_i for each ion (found from single-salt experiments) are needed to calculate the expected conductance from the Läuger theory. However, attempts to use this theory to calculate the expected conductance of the SR channel in mixtures were not successful when thallous ion was included in the solution (Fox, 1983). Our model is capable of accounting for the effects of thallous ion, as will be shown in this section.

Representative pairs of current records are shown in Fig. 5 to illustrate these effects. The marked decrease in the channel conductance upon

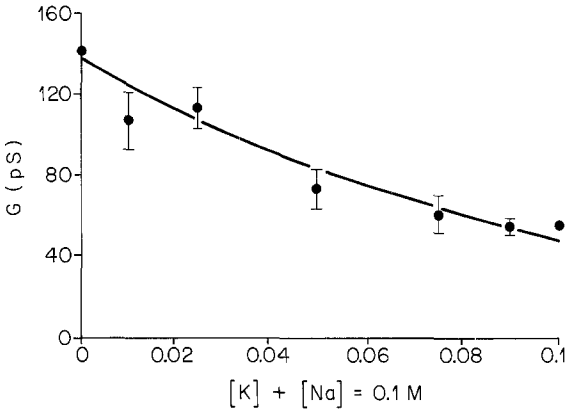

Fig. 4. Conductance in mixtures of potassium and sodium sulfate at 0.2 M total concentration. Each point is the average of the conductances found at low voltage for the indicated mixed solutions. The curve is drawn according to the equation derived from Läuger's single-ion theory for two-salt mixtures (Läuger, 1973). The data are plotted as conductance versus mole fraction of sodium

replacement of only 10% of the potassium ions by thallous ions is quite evident (note the different scales for the traces). These effects were found at each of the four total ion concentrations used for potassium-thallium mixtures, and at both concentrations of ammonium-thallium mixtures (reported previously in Fox, 1983). Experimental results with sodium were consistent with a minimum in the conductance near 10% thallium at both 0.1 and 1 M total

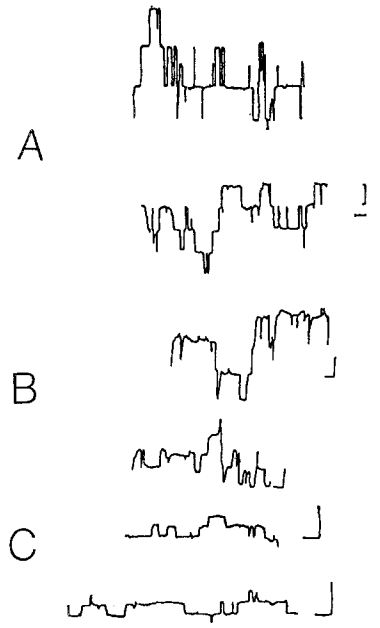

Fig. 5. SR channel current steps in pure acetate salts of K^+, NH_4^+ and Li^+, as well as in mixtures of these salts with thallium acetate, in a molar ratio of 9 : 1. All experiments were done in symmetric solutions, with 90% PE-10% PC decane-containing membranes. Horizontal scale: 15 sec for all records. *A*. 0.5 M potassium acetate (top trace); 0.45 M potassium, 0.05 M thallium acetate (bottom trace). Vertical bar: 100 pS. *B*. 0.1 M ammonium acetate (top trace); 0.09 M ammonium, 0.01 M thallium acetate (bottom trace). Vertical bar: 100 pS. *C*. 0.5 M lithium acetate (top trace); 0.45 M lithium, 0.05 M thallium acetate (bottom trace). Vertical bar: 25 pS (top), 50 pS (bottom)

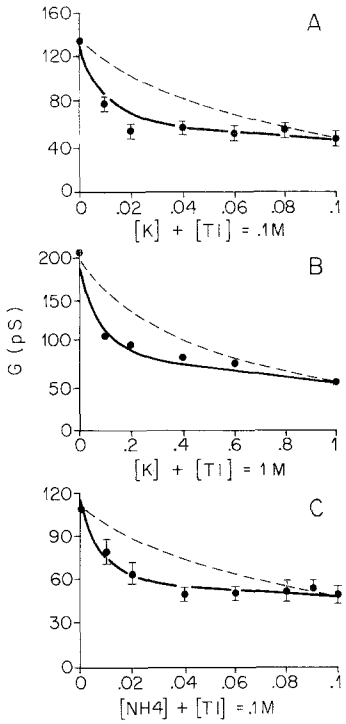

Fig. 6. SR channel conductance in symmetric mixed (acetate salt) solutions of thallium with either potassium (*A*, 0.1 M; *B*, 1 M) or ammonium (*C*, 0.1 M) at fixed total concentrations. The data are plotted as conductance versus mole fraction of thallium; each point represents the average of the channel conductances found at low voltage. Membranes were of 90% PE-10% PC in decane. Continuous curves are from our model, while the dashed curves illustrate the predictions of the Läuger model. The constants used to fit these curves are listed in Table 2; for the Läuger model, only the binding constant and the (unbound) g^{max} are used

concentrations, as fitted by our model, although the minimum conductance was within one standard deviation of the maximum conductance at 0.1 M sodium (Fox, 1984).

Small percentages of thallous ion had the opposite effect on the conductance in mixtures of lithium and thallium. Since the maximum channel conductance for thallium is greater than for lithium, Läuger's theory does predict an increase in channel conductance as the mole fraction of thallium increases in mixtures. However, a much greater increase than predicted by that theory was found at low mole fractions of thallium. Our results are illustrated by the pair of current traces for 0.5 M LiAc and 0.45 LiAc − 0.05 TlAc in Fig. 5*C*, and a plot of the prediction of our model to this data is shown in Fig. 7. This effect, an enhancement of channel conductance, has not been seen before in investigations of thallium interactions with other cation channels.

SR channel conductance was also studied as a function of total concentration in mixed solutions with a constant mole fraction of thallous ion. Figure 8 shows channel conductance in mixed 90% potassium-10% thallium acetate solutions at total salt concentrations varying from 0.03 to 1 M.

The results of these experiments are presented in Figs. 6 through 8 along with the theoretical curves [from Eq. (1)] fit to the data. All experiments were done in symmetric solutions.

Competition Experiments

In order to better characterize the inhibitory effect of thallium on the potassium conductance of the SR channel, we performed experiments in which the channel conductance was measured as a function of the potassium concentration in the presence of a constant concentration of thallium. These experiments are analogous to those used to determine the mechanism of inhibitor action in enzyme systems, if thallous ion is thought of as the inhibitor and potassium as the substrate.

The results of these competition experiments, shown with a double-reciprocal plot in Fig. 9 are fit well by the curve illustrating Eq. (1). The total concentration is different for each point in the Figures shown here, unlike the case for the Figures shown in the preceding section, where the total concentra-

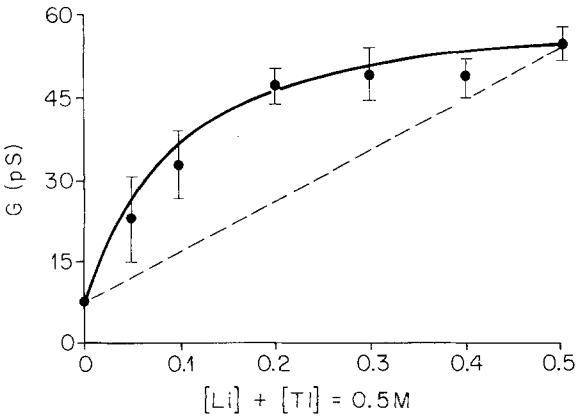

Fig. 7. SR channel conductance in symmetric mixed solutions of thallium and lithium acetate at a total concentration of 0.5 M is plotted as function of thallium concentration. Membranes were composed of 90% PE-10% PC in decane. Data points represent the average of the channel conductances at low voltage. The continuous curve is drawn according to our model, while the dashed curve represents the prediction of the Läuger model

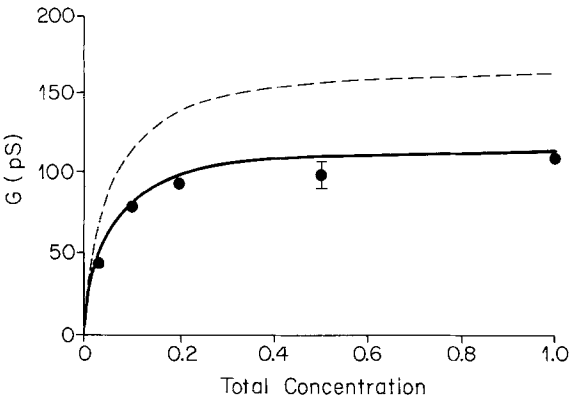

Fig. 8. SR channel conductance in symmetric mixed potassium and thallium acetate solutions, each composed of 90% potassium, 10% thallium, is plotted versus the total concentration of the mixture in moles per liter. The conductance is the average single-channel conductance at low voltage; membrane composition was PE-PC in decane. The continuous curve represents the prediction of our model, while the dashed curve represents that of Läuger's model. These curves are plotted with the constants listed in Table 2

tion was constant throughout each experiment. In Figs. 9*A* and 9*B* the data for channel conductance in potassium acetate without thallium is also presented (the straight lines) for comparison.

Current-Voltage Relations in Thallous and Mixed Potassium-Thallous Ion Solutions

In this section we describe single-channel current-voltage relationships in the presence of thallous ion, either as the only cation in solution (Fig. 10) or in a mixture of thallium with potassium acetate (Fig.

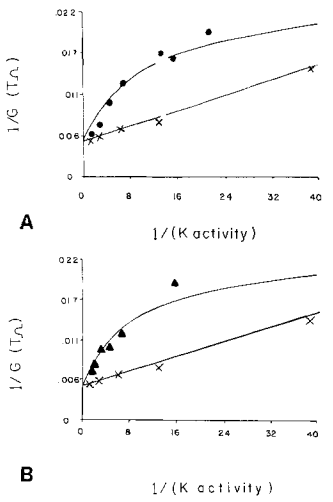

Fig. 9. Double-reciprocal plot of SR channel conductance in symmetrical mixed solutions containing constant concentrations of thallium with various potassium concentrations is shown. Membranes were PE-PC in decane. The concentration of potassium varied from 0.02 to 1 molar. In *A* thallium concentration is 0.04 M; in *B* thallium concentration is 0.05 M. Potassium activity is from Robinson and Harned (1941). The theoretical curve, illustrating our model, is plotted using the constants in Table 2. The circles indicate experimental points for mixed potassium-thallium solutions, with potassium concentration varying, while the x's indicate the channel conductance in potassium solutions with no added thallium

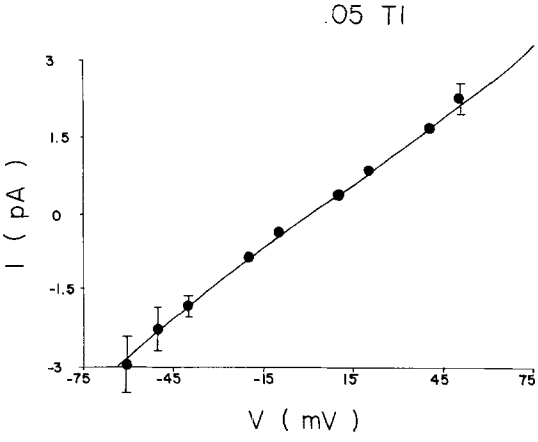

Fig. 10. SR channel conductance in pure thallium acetate solutions is plotted as a function of voltage. The membrane was PE-PC in decane; thallium acetate concentration was 0.05 M. The curve indicates the prediction of our model

11). The curves are calculated from Eq. (5) (multiplying it by the voltage). They are very nearly linear, particularly over the range (±50 mV) where most of the measurements were taken.

In mixtures, deviations from linearity in the *I-V* plot of up to 30% greater conductance at high voltage than near zero voltage were observed, as shown in Fig. 11. The greatest deviation from linearity occurred at negative voltages, where a degree of

Table 1.[a] A. Zero Current Potentials and Permeability Ratios at Several Concentrations

[ ]	*cis*	*trans*	V_0(exp.)	V_0(calc.)	P_T/P_{ion}
0.01	K	Tl	19.0 ± 1.6 (3)	17.6	2.11
0.01	Tl	K	−18.2 ± 0.39 (3)	−21.5	2.05
0.1	K	Tl	17.0 ± 1.0 (3)	17.3	1.95
0.1	Tl	K	−20.8 ± 1.2 (2)	−21.2	2.27
0.5	K	Tl	19.6 ± 0.48 (4)	17.3	2.16
0.7	K	Tl	22.8 ± 1.8 (5)	17.3	2.45
1.0	K	Tl	19.8 ± 0.92 (4)	17.3	2.18
0.1	Li	Tl	59.3 ± 4.2 (3)	59.0	10.33
1.0	Li	Tl	58.7 ± 1.7 (2)	59.0	10.08

B. Calculated Permeability Ratios as a Function of Thallium Mole Fraction

% Tl	10	20	30	40	60	80	100
P_T/P_K	4.2	4.8	3.2	2.6	2.2	2.1	2.3

[a] Zero-current potentials were determined from *I-V* plots of single-channel currents observed under bi-ionic conditions (equal concentrations of the two salts on either side of the membrane). These values are presented under the heading V_0(exp.). The zero-current potential predicted by our model is listed under the heading V_0(calc.). All zero-current potentials are reported in mV. The permeability ratios were calculated from the relation

$$P_T/P_K = e^{V_0F/RT}$$

where RT/F is 25.4 mV at 22°C, and P_K represents either potassium or lithium. The lower section of the Table presents the permeability ratios calculated from the zero-current potentials shown in Fig. 12.

asymmetry in the *I-V* relation can also be seen, with larger channel currents when the *cis* pool is negative than when it is positive. This behavior was most apparent in mixed solutions. It is fit by the model with the assumption that the exit rates for ions in the channel are different, with exit to the *cis* pool favored over the exit to the *trans*.

V_0 *Experiments*

Table 1 lists the results of experiments which measured zero-current potentials V_0 at several concentrations for the ions K and Li versus Tl. These measurements were done under bi-ionic conditions, with the zero-current potential determined from single-channel current-voltage plots. V_0 is nearly constant over the concentration range 0.01 to 1 M for potassium and thallium, and is also nearly the same for lithium and thallium at 0.1 M and at 1 M. The permeability ratios were calculated without correcting for activity. If activity corrections had been used, they would not be constant, but would range

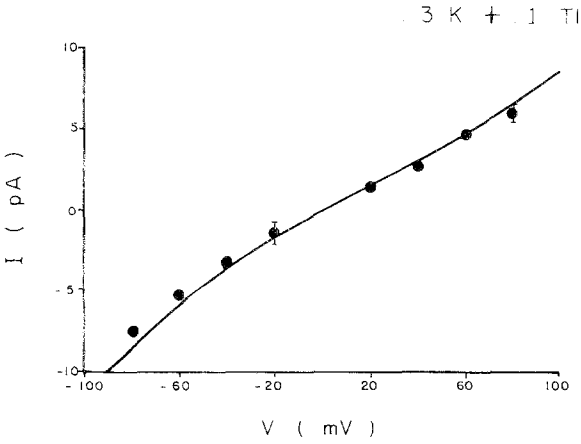

Fig. 11. SR channel current in a symmetric 0.6 M K-0.1 M Tl (acetate salt) mixture is shown as a function of the applied voltage. A Montal membrane composed of PE-PS was used for this experiment. The curve indicates the prediction of our model

from 2.12 at 0.01 M to 3.3 at 1 M (for the ratios P_T/P_K; Fox, 1983). The absolute value of the zero-current potentials does not depend greatly upon which end of the channel faces the thallium-containing solution, consistent with the assumption that there is one modulatory site on both sides of the membrane. This is seen in the V_0 measurements at 0.01 and at 0.1 M concentration under bi-ionic conditions.

Figure 12 shows the behavior of V_0 when the mole fraction of thallium was varied in mixed Tl^+-K^+ solutions on the *cis* side of the membrane (at a total concentration of 0.1 M), while the solution on the *trans* side was 0.1 M KAc for all experiments. The zero-current potential with Tl^+ on the *cis* side only goes to −20.8 mV as the mole fraction of thallium approaches 100%. The theoretical curve is from the G-H-K equation with permeability ratios given by Eq. (9). The same asymmetry in the exit rates that has been used to account for the *I-V* behavior is appropriate to fit this data as well, which is particularly pleasing since the fit here would not be nearly so good if the exit rate ratios were taken to be one. At the same time, this asymmetry in exit rates does not lead to a prediction of a large asymmetry in the bi-ionic potentials, in agreement with the data.

In a simple one-ion channel, under conditions near to equilibrium, the permeability ratio for any two ions should be given by the ratio of their maximum conductances multiplied by the ratio of their binding constants (Hille, 1975). If this calculation is carried out in our case, potassium is expected to be the more permeant ion (the ratio P_T/P_K estimated in this way is 0.82). An interesting feature of the results presented here is that the permeability ratios indicate that thallium is the more permeant ion ($P_T/$

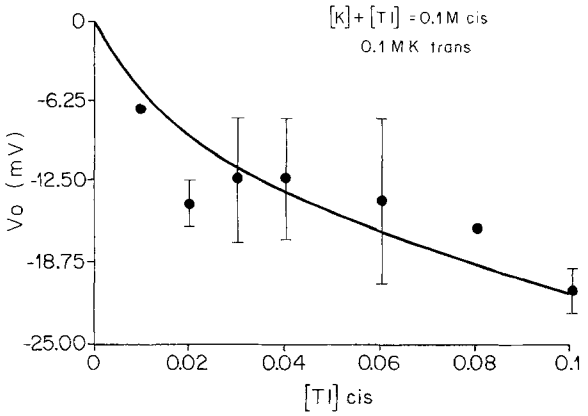

Fig. 12. Zero-current potentials across SR channels incorporated into PE-PC decane membranes separating asymmetric solutions are shown. The *trans* pool contained 0.1 M potassium acetate in each experiment, while the solution in the *cis* pool contained mixed potassium and thallium acetate at a total concentration of 0.1 M. The measured zero-current potentials are plotted as a function of the thallium mole fraction in the *cis* pool; the theoretical curve is plotted with the constants listed in Table 2

P_K greater than one, as deduced from the zero-current potential under conditions near equilibrium). Although we will discuss this point more fully in the Discussion section, it should be noted that this discrepancy is compatible with our model.

Discussion

Assumptions of the Model

The basic findings which must be accounted for in order to successfully model our results include anomalous mole fraction effects on conductance, discrepancies between permeability and conductance ratios, and slightly hyper-linear current-voltage relations.

The model which we propose in order to fit our data is based on the idea that thallium binds to a modulatory site, thereby altering the properties of the SR channel. Some of the assumptions we make, although inevitably arbitrary, are generally consistent both with properties inferred from previous work on this channel, and with previously proposed interpretations of the anomalous effects of thallous ion on other channels (Hagiwara et al., 1977; Sandblom et al., 1977; Krasne et al., 1983). For example, the assumption that the channel may only contain one permeant ion at a time follows from the work of Coronado et al. (1980), which shows that the behavior of the conductance and of the zero-current potential is consistent with the predictions of Läuger's single-ion pore theory (Läuger, 1973).

In the presence of thallous ion our theory is more complex than that of Läuger, and does not necessarily predict simple saturating behavior of the conductance. However, due to the very large thallium binding constant to the modulatory site, Eq. (1) becomes virtually the same as Läuger's in single-salt solutions. This is because the contribution to the conductance due to the unbound state becomes negligible when the product $K_B C_T$ is large, as it is in this case for all of the experimental conditions, whereas the fraction expressing the contribution by the altered state is virtually one. Accordingly, the shape of the curve shown in Fig. 3 is as expected for a single-ion channel. That the channel behaves like a single-ion channel even in mixed solutions, where the anomalous mole fraction effects are most noticeable, is suggested by the finding that the conductance versus (total ion) concentration curve in mixed 90% potassium-10% thallium acetate has a shape similar to that for pure thallium (Fig. 8). As in Fig. 3, there is no indication of a decrease in conductance, even at high concentrations, where such effects might be evident if the channel were doubly occupied. These considerations, in conjunction with the finding that the bi-ionic zero-current potential varies little with ion concentration (Table 1) suggest that the available evidence is compatible with the one-ion channel assumption.

The hypothesis that the binding constant to the modulatory site is independent of the state of occupancy of the pore (assumption 6 in Appendix A) is introduced mainly to reduce the number of parameters, but is not indispensable to fit the data. A fortunate consequence of this assumption, however, in that it greatly simplifies the analysis, is that the depth of the internal well (and therefore the binding constants of the various ions to the well) is unaltered by binding to the external site, so that the sole permeation parameter modified by thallous ion binding to the modulatory site is the maximum conductance. This circumstance can easily be proven using microscopic reversibility.

The assumption that cations other than thallous may compete for the modulatory site is required in order to fit the competition experiments, but is also very reasonable in that a site which binds thallium ion is naturally expected to have some affinity for other cations as well.

The discrepancy between the permeability ratio and the conductance ratios in single-salt solutions is accounted for by the hypothesis that the channel is altered by thallous ion binding. More specifically, the expression for the permeability ratio, Eq. (9), contains parameters, such as $g_{BK}^{\max}$, which are not deducible from conductance measurements in single-salt conditions, implying that in this model the two quantities are generally not relatable.

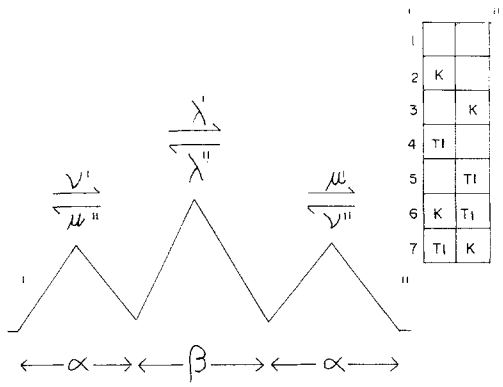

Fig. 13. Energy barrier model for a two-site pore, as discussed in Appendix B. The diagram enumerates the seven possible occupancy states of the channel if double occupancy is only allowed for unlike ions

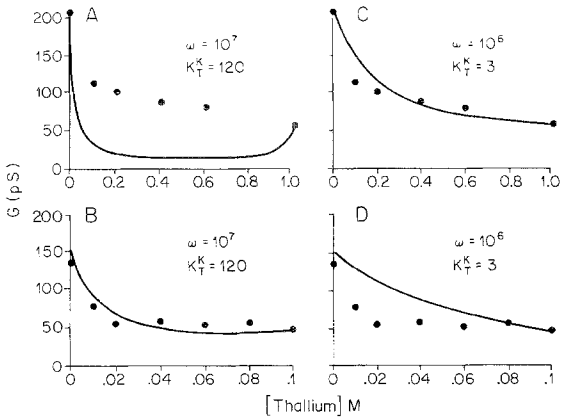

Fig. 14. These figures illustrate our attempts to fit the conductance data from mixed solution experiments using the double occupancy model described in Appendix B. Values of the constants which give reasonable fits to the experimental data at one total concentration will not give reasonable fits to the experimental data at other concentrations, as is illustrated in the paired plots in this Figure. *A* and *C* plot the conductance data for mixed potassium-thallium at 1 M total concentration, while *B* and *D* plot the data for 0.1 M total concentration. (The fit of our model to this data was presented in Fig. 6.) In *A* and *B*, we show the prediction of Eq. (B7) with the values $W = 10^7$ and $K_T^K = 120$. With these values, the double-occupancy model fits the experimental data for 0.1 M total concentration, but does not fit the data for 1 M total concentration. With the values $W = 10^6$ and $K_T^K = 3$, the model now fits the data for 1 M total concentration, but does not fit the data for 0.1 M (shown in *C* and *D*)

Alternative Models

SR channel conductance in mixed potassium- or ammonium-thallium acetate solutions was fitted in a previous report (Fox, 1983) using an equation proposed by Neher (1975) for describing the effects of thallous ion on gramicidin conductance. However, the observed conductance in lithium-thallium acetate mixtures could not be fit by this equation, which, at any rate, is an empirical equation restricted to the zero-current conductance that cannot be extended in any obvious way to derive the expected permeability ratio or the current-voltage relation.

An alternative attempt to fit our data consisted of applying a model recently elaborated by Läuger, Stephan and Frehland (1980), in which the kinetics of channel fluctuation is allowed to interact with that of permeation. This model is particularly attractive, because it is based on very reasonable assumptions and is known to predict certain results similar to those expected for multi-ion pores. Extending the results of Läuger et al. (1980) to the case of two ions (Ciani, 1984), we derived expressions for the conductance as well as for the zero-current potential. However, using the predictions of this model for the conductance, it was found to be impossible to fit the data from mole fraction conductance experiments at more than one total concentration with the same constants.

Similar problems were encountered in attempts to fit our data with equations derived for models which allowed for multi-ion occupancy of the channel. Several cation channels are thought to be occupiable by more than one ion at a time. Among these are gramicidin (Eisenman et al., 1977; Urban et al., 1978) and various potassium channels found in nerve, muscle and egg cell membranes (*see* Hille & Schwarz, 1978 for a comprehensive review and discussion). Models for doubly or multiply occupied pores may predict anomalous mole fraction effects, maxima in the conductance versus concentration relation, and deviation of the flux ratio from the Ussing-Teorell criterion. To determine whether such models might be applicable to our results with the SR channel, we have deduced an equation for the conductance of a two-site channel, schematically illustrated in Fig. 13, assuming that it may be either empty, singly occupied or doubly occupied by one K^+ and one Tl^+ ion, but not by two ions of one species. (We do not include double occupancy by two like ions since no conductance maxima are apparent in single-salt solutions.) This model is derived in Appendix B. The results of our attempts to fit the conductance data are illustrated in Fig. 14, where we show that we have been unable to find a set of values for the constants which would simultaneously fit the data at different concentrations. (The fit of our model to this data was presented in Fig. 6.) We thus are led to infer that the postulate of double-ion occupancy is not easily reconcilable with the observed conductance behavior of the SR channel.

Table 2. Model parameters used to fit the experimental data[a]

Maximum conductances (pS):		
Ion	Unbound	Bound
Tl	250	57.5
K	212	80
NH_4	168	65
Li	7.7	15
Binding constants:		
Ion	Internal	Modulatory
Tl	54.8 M^{-1}	K_{BT} = 14,000 M^{-1}
K	18.2 M^{-1}	K_{BK} = 1500 M^{-1}
NH_4	27.3 M^{-1}	K_{BK} = 1500 M^{-1}
Li	52.6 M^{-1}	K_{BLi} 5000 M^{-1}
Channel Parameters:		
R_T	0.7	
R_K	0.6	
alpha	0.5	
beta	0.5	

[a] These values were used to generate the curves in the Figures showing our model predictions. The value we use for the unbound maximum conductance for K^+ is very similar to the maximum conductance value reported by Bell and Miller (1983). We have used the maximum channel conductances values reported by Coronado et al. (1980) for NH_4^+ and Li^+ as the unbound maximum conductances for these ions. For both K^+ and NH_4^+, the best value for the binding constant to a modulatory site, K_{BK}, was 1500 M^{-1}, while the best value for the binding of lithium to a modulatory site was 5000 M^{-1}. The values of alpha and beta indicate the placement of the internal site in the center of the voltage drop across the membrane.

Assignment of Parameter Values

The constants which appear in Eqs. (1) through (10) of the Results section were fit to the data with computer programs which used a wide range of possible values for the constants in the preceding equations, and saved those which minimized the square of the difference between the calculated and the experimental values. These values are presented in Table 2. The strategy used to make this fitting is described in the following paragraphs.

The g_K^{max} and K_k values for potassium were evaluated from the results of experiments performed at various concentrations of potassium salt.

Like the potassium data, the data from thallium salt experiments were well fit by a simple model with a single site of permeation. Our expression for SR channel conductance [Eq. (1)] in pure Tl^+ salts becomes virtually indistinguishable from that expected for such model if the value of the binding constant to the modulatory site is so large that the probability of its being occupied at the concentrations used is virtually one. Assuming this to be the case, we could then identify the g^{max} found from single thallium salt experiments as the g_{BT}^{max}, namely the maximum conductance to thallium of the bound channel. The binding constant of Tl^+ to the internal site K_T, can be found directly from single thallium salt experiments, since according to our model it is not altered by the state of occupancy of the modulatory site.

We initially tried to fit our data with models which assumed that only thallous ion could bind to the modulatory site. These attempts were not successful. However, by introducing the reasonable idea that potassium (or, in general, any other cation) could compete with thallium for binding to the modulatory site, we were able to fit both the mole fraction and the competition experiments with a consistent set of constants. Values for K_{BT} and K_{BK} were found by fitting the results of the mole fraction and competition experiments simultaneously.

The nonlinearities and asymmetries found in the *I-V* relations could be fit by adjusting either the ratios R_T and R_K, or the values of alpha and beta, (which determine the position of the internal site in the potential field), or both. For simplicity, and also because the limited degree of asymmetry in the experimental range of voltage did not allow us to clearly distinguish between the three alternative possibilities, we assumed that the internal site was centered, by setting alpha equal to beta, and varied the rates R_K and R_T. Using the R_T and R_K values fit to the *I-V* data alone, we determined the best value of g_T from the mole fraction V_0 data. As can be seen from the Figures, the final set of values determined in this way gives good fits to all of our experimental data.

Activity Corrections

The permeability ratios calculated from bi-ionic potentials listed in Table 1 do not vary much with concentration, in agreement with the model. If, however, activity corrections are used, the calculated values do show some variation. For example, the permeability ratio P_T/P_K deduced using activity corrections is 2.12 at 0.01 M, while at 1 M it is 3.31. Although the use of activities is certainly correct in the case of reversible electrodes, the theoretical basis for applying them to the bi-ionic case is not entirely clear. For example, in the equations for the flux through the pore (irrespective of binding to the modulatory sites), the aqueous compositions appear in the equations through the rate constants, $\nu = \rho c$, or $\nu = \rho a$, where c and a are presumably proportional to the number of ions ready to jump into the channel, and ρ is assumed to be constant. It is not evident that the use of bulk solution activities

in the definition above is any less arbitrary than the use of concentration, or provides better assurance that ρ is independent of concentration. Moreover, the difficulty of doing V_0 measurements in single-channel experiments implies sufficient uncertainty that it is difficult to use this data to discriminate between possible models.

Conclusions

We conclude from the results presented that:
1) Thallous ion is permeant in the SR channel. Channel conductance saturates with increasing thallous ion concentration, and does not decline from its maximum level even at concentrations up to fifty times greater than the half-maximal.
2) SR channel conductance in mixed solutions of thallous ion with potassium, ammonium, or sodium ions is less than predicted by the simple single-ion theory of Läuger, but is greater than predicted by that theory in mixed thallous and lithium ion solutions. The channel conductance in mixed sodium-potassium solutions is well described by the theory of Läuger.
3) An anomaly is also found in that, although SR channel maximum conductance in thallium acetate solutions is less than in potassium acetate, and the product of the ion binding constants and maximum conductances from single-salt experiments would indicate that potassium is more permeant than thallium (assuming a simple single-ion pore), zero-current voltage measurements indicate that thallous ion is more permeant than potassium.
4) The current-voltage relations in pure thallium acetate and in mixed thallium-potassium acetate solutions are both somewhat nonlinear and asymmetric, with greater conductance when the potential of the solution to which the vesicles are added is negative.
5) The effects of thallous ion on channel conductance are accounted for in a quantitative manner by the model presented, which postulates external modulatory sites to which one thallous ion may bind, thereby altering the maximum conductance of the channel to the cations in solution by modifying the barriers of the pore. Other cations compete with thallous ion for binding to these modulatory sites, but only thallous ion binding affects the permeability properties of the channel. The channel is assumed to have one internal site, and thus to be a one-ion pore. The discrepancy between the permeability ratios calculated in the two ways described in conclusion 3) is reconciled within the framework of the model by the decrease of the maximum conductance to potassium in the altered state of the channel.

We wish to thank Dr. S. Krasne for experimental suggestions and useful discussions. J.F. received support from NIH grant GM07191-08. This research was supported by a grant from the Muscular Dystrophy Association.

References

Anderson, O. 1975. Ion-Specificity of Gramicidin Channels. *Abstract, Int. Biophys. Congr.*, Copenhagen, 112

Ashcroft, F., Stanfield, P. 1983. The influence of the permeant ions thallous and potassium on inward rectification in frog skeletal muscle. *J. Physiol. (London)* **343**:407–428

Bell, J., Miller, C. 1983. Effects of Phospholipid Surface Charge on Ion Conduction in the K^+ Channel of the Sarcoplasmic Reticulum. *Fourth Biophysical Discussion.* (published by the Biophysical Society) pp. 223–228. Airlie House, Airlie (Virginia)

Ciani, S. 1984. Coupling between fluxes in one-particle pores with fluctuating energy profiles. A theoretical study. *Biophys. J.* **46**:249–252

Ciani, S., Krasne, S., Miyazaki, S., Hagiwara, S. 1978. A model for anomalous rectification: Electrochemical-potential-dependent gating of membrane channels. *J. Membrane Biol.* **44**:103–134

Coronado, R., Miller, C. 1979. Voltage-dependent cesium blockade of a cation channel from fragmented sarcoplasmic reticulum. *Nature (London)* **280**:807–810

Coronado, R., Miller, C. 1980. Decamethonium and hexamethonium block K^+ channels of the sarcoplasmic reticulum. *Nature (London)* **288**:495–497

Coronado, R., Miller, C. 1982. Conduction and block by organic cations in a K^+-selective channel from sarcoplasmic reticulum incorporated into planar phospholipid bilayers. *J. Gen. Physiol.* **79**:529–547

Coronado, R., Rosenberg, R., Miller, C. 1980. Ionic selectivity, saturation, and block in a K^+ channel from sarcoplasmic reticulum. *J. Gen. Physiol.* **76**:425–446

Eisenman, G., Sandblom, J., Neher, E. 1977. Ionic selectivity, saturation, binding, and block in the gramicidin A channel: A preliminary report. *In:* Metal-Ligand Interactions in Organic Chemistry and Biochemistry. B. Pullman and N. Goldblum, editors. Pt. 2, pp. 1–36. Reidel, Dordrecht

Fox, J. 1983. Thallous ion permeation through the cation-selective channel of the sarcoplasmic reticulum: Anomalous mole fraction dependence. *Biochim. Biophys. Acta* **736**:241–245

Fox, J. 1984. Thallous ion interactions with the cation selective channel of the sarcoplasmic reticulum. Ph.D. Dissertation, U.C.L.A., Los Angeles, California

Gay, L. 1981. Thallium and the potassium permeability mechanism of resting frog sartorius muscle. *J. Physiol. (London)* **312**:39P

Hagiwara, S., Eaton, D.C., Stuart, A.E., Rosenthal, N.P. 1972. Cation selectivity of the resting membrane of squid axon. *J. Membrane Biol.* **9**:373–389

Hagiwara, S., Miyazaki, S., Krasne, S., Ciani, S. 1977. Anomalous permeabilities of the egg cell membrane of starfish in K^+-Tl^+ mixtures. *J. Gen. Physiol.* **70**:269–281

Hagiwara, S., Takahashi, K. 1974. The anomalous rectification and cation selectivity of the membrane of a starfish egg cell. *J. Membrane Biol.* **18**:61–80

Hamill, O.P., Marty, A., Neher, E., Sakman, B., Sigworth, F.J. 1981. Improved patch-clamp techniques for high-resolution current record from cells and cell-free membrane patches. *Pfluegers Arch.* **391**:85–100

Hille, B. 1973. Potassium channels in myelinated nerve. *J. Gen. Physiol.* **61**:669–686

Hille, B. 1975. Ionic selectivity of Na and K channels of nerve membranes. *In:* Membranes—A Series of Advances. G. Eisenman, editor. Vol. 3, pp. 255–323. Dekker, New York

Hille, B., Schwarz, W. 1978. Potassium channels as multi-ion single-file pores. *J. Gen. Physiol.* **72**:409–442

Hladky, S., Urban, B., Haydon, D. 1979. Ion movements in pores formed by gramicidin A. *In:* Membrane Transport Processes. C. Stevens and R. Tsien, editors. pp. 89–103. Raven, New York

Krasne, S., Ciani, S., Hagiwara, S., Miyazake, S. 1983. A model for ion-composition-dependent permeabilities of K^+Tl^+ during anomalous rectification. *In:* The Physiology of Excitable Cells. A. Grinnel and W. Moody, editors. pp. 83–97. Alan R. Liss, New York

Labarca, P., Coronado, R., Miller, C. 1980. Thermodynamic and kinetic studies of the gating behavior of a K^+-selective channel from the sarcoplasmic reticulum membrane. *J. Gen. Physiol.* **76**:397–424

Läuger, P. 1973. Ion transport through pores: A rate theory analysis. *Biochim. Biophys. Acta* **311**:423–441

Läuger, P., Stephan, W., Frehland, E. 1980. Fluctuation of barrier structure in ionic channels. *Biochim. Biophys. Acta* **602**:167–180

Miller, C. 1978. Voltage-gated cation conductance channel from fragmented sarcoplasmic reticulum: Steady-state electrical properties. *J. Membrane Biol.* **40**:1–23

Miller, C. 1982*a*. Feeling around inside a channel in the dark. *In:* Transport in Biomembranes. R. Antolini, editor. pp. 99–108. Raven, New York

Miller, C. 1982*b*. Bis-quaternary ammonium blockers as structural probes of the sarcoplasmic reticulum K^+ channel. *J. Gen. Physiol.* **79**:869–891

Miller, C. 1983. Integral membrane channels: Studies in model membranes. *Physiol. Rev.* **63**:1209

Miller, C., Racker, E. 1976. Ca^{++}-induced fusion of fragmented sarcoplasmic reticulum with artificial planar bilayers. *J. Membrane Biol.* **30**:283–300

Miller, C., Rosenberg, R. 1979*a*. A voltage-gated cation conductance channel from fragmented sarcoplasmic reticulum; Effects of transition metal ions. *Biochemistry* **18**:1138–1145

Miller, C., Rosenberg, R. 1979*b*. Modification of a voltage-gated K^+ channel from sarcoplasmic reticulum by a pronase-derived endopeptidase. *J. Gen. Physiol.* **74**:457–478

Neher, E. 1975. Ionic specificity of the gramicidin channel and the thallous ion. *Biochim. Biophys. Acta* **401**:540–544

Neher, E., Sandblom, J., Eisenman, G. 1978. Ionic selectivity, saturation, and block in gramicidin A channels. II. *J. Membrane Biol.* **40**:97–116

Robinson, R., Harned, H. 1941. Some aspects of the thermodynamics of strong electrolytes from electromotive force and vapor pressure measurements. *Chem. Rev.* **28**:419–477

Sandblom, J., Eisenman, G., Neher, E. 1977. Ionic selectivity, saturation, and block in gramicidin A channels. I. Theory for the electrical properties of ion selective channels having two pairs of binding sites and multiple conductance states. *J. Membrane Biol.* **31**:383–417

Urban, B., Hladky, S., Haydon, D. 1978. The kinetics of ion movements in the gramicidin channel. *Fed. Proc.* **37**:2628–2632

Received 3 April 1984; revised 26 June 1984

Appendix A

The model we propose is based on the idea that thallous ion binding to one of two postulated external binding sites on the SR channel will alter the permeability properties of the channel. We will describe the ionic fluxes by Eyring rate theory, and the pore will be modeled as one internal site separated from the aqueous solutions by two lateral energy barriers, as shown in Fig. 1. The description of ion transport is based on a number of assumptions, most of which, however, should not be considered indispensable to account for our data, but rather as necessary to reduce the number of parameters and formulate the simplest adequate model. These assumptions are as follows:

1) The SR channel can be schematized by two energy barriers with a site in between.

2) In addition to the internal well, the channel has two external cation binding sites, one on each side. Thallous ion binding to one of these sites causes an alteration in the permeability properties of the pore, although the relative heights of the energy barriers, and the location of the peaks and of the internal well are unaffected.

3) Other cations may compete with thallous ion for binding to these sites, but their binding does not affect the transport properties of the pore.

4) Only one modulatory site per channel may be bound at a time, and the channel alteration due to thallous ion binding does not depend on whether binding is to the *cis* or *trans* site.

5) Ion association and dissociation to the external sites are considered to be so fast that bound and unbound channels in the same state of internal occupancy are at equilibrium with each other.

6) The binding constants to the external sites are independent of the occupation of the pore, being the same for an empty channel as for an internally occupied one.

From assumptions 1) to 4) and considering a channel with a cation bound to the left external site as indistinguishable from one with the same cation bound to the right external site, it is easy to see that the pore can exist in $(n + 1)^2$ different states, with n being the number of cations in the system. Since n is at most equal to 2 in the mixtures being considered, there will be at most nine states. The number of pores (per unit area of membrane) in each of these states can be subdivided as follows:

N (unbound, empty)

N_i (unbound, occupied by cation i) (i = 1, 2)

N_{Bl} (bound by cation l, empty) (l = 1, 2)

$N_{Bl,i}$ (bound by cation l, occupied by cation i) (i,l = 1, 2).

Bound and unbound states will be related by the conditions for equilibrium:

$$N_{Bl} = K_{Bl}N(C_l' + C_l''); \; N_{Bl,i} = K_{Bl}N_i(C_l' + C_l'') \qquad \text{(A1)}$$

where the equilibrium constant K_{Bl} is the same in the two equa-

tions on account of assumption 6). Moreover, due to assumption 5), Eqs. (A1) are assumed to hold even when the equilibrium of the overall system is perturbed by ion movement through the channel. If K^+ and Tl^+ are the two species of cations present, and using Eq. (A1) to relate bound and unbound pores, the total number of channels per unit area, N^T will be given by

$$N^T = [N + N_K + N_T] \cdot [1 + K_{BK}(C'_K + C''_K) + K_{BT}(C'_T + C''_T)]. \quad \text{(A2)}$$

Equation (A2) will give us the sum $N + N_K + N_T$, while the separate values for N, N_K and N_T will be provided by Eq. (A2) in conjunction with the steady-state conditions

$$\frac{dN_K}{dt} = \frac{dN_T}{dt} = 0. \quad \text{(A3)}$$

Since N_K and N_T are assumed to be at equilibrium with their corresponding bound states, the rate-limiting step in the kinetics of variation of N_K and N_T will be that of ion permeation, so that Eq. (A3) can be written

$$\frac{dN_K}{dt} = \nu_K N - \mu_K N_K = 0;$$

$$\frac{dN_T}{dt} = \nu_T N - \mu_T N_T = 0 \quad \text{(A3')}$$

where ν_i and μ_i are defined by

$$\nu_i = \nu'_i + \nu''_i \quad (i = K, T)$$
$$\mu_i = \mu'_i + \mu''_i \quad \text{(A4)}$$

while the meaning of the individual rate constants should be clear from Fig. 1. From Eqs. (A1), (A2) and (A3') the number of channels in each of the nine states can be calculated simply. (It should be mentioned that instead of Eqs. (A3') we could have used the corresponding equations for N_{BK}, $N_{BK.K}$, $N_{BK.T}$, $N_{BT.K}$, and $N_{BT.T}$ and similarly, Eq. (A2) could have been written in terms of one of these triplets. It is easy to prove that assumption 5) and the stipulation in assumption 2) that binding of Tl^+ does not alter the relative heights of the two barriers would give us the same results for the nine values of the N's.)

Expressions for the Fluxes

Since we assume that the channel properties are changed only when Tl^+ is bound to a modulatory site, the rate constants for each modified channel will be indicated by ν_{Bi} (instead of $\nu_{BT.i}$), where B stands for "bound by Tl^+" and i denotes, as before, the permeant cation. At steady state, the total flux of potassium and thallium ions will be

$$J_K = [\nu'_K(N + N_{BK}) - \mu''_K(N_K + N_{BK.K})] + [\nu'_{BK}N_{BT} - \mu''_{BK}N_{BT.K}] \quad \text{(A5)}$$

and

$$J_T = [\nu'_T(N + N_{BK}) - \mu''_T(N_T + N_{BK.T})] + [\nu'_{BT}N_{BT} - \mu''_{BT}N_{BT.T}]. \quad \text{(A6)}$$

All the equations in the text are obtained by adding (A5) to (A6), replacing the rate constants by their explicit expressions in terms of potential and ion concentrations:

$$\nu' = \mu' C' e^{\alpha u/2},\ \mu' = \mu' e^{\beta u/2},\ \nu'' = \mu'' C'' e^{\beta u/2},\ \mu'' = \bar{\mu}'' e^{\alpha u/2} \quad \text{(A7)}$$

and substituting the N's by their explicit expressions as obtained by Eqs. (A1), (A2) and (A3'). We have also made use of the four relations:

$$\bar{\rho}'_i\bar{\mu}''_i = \bar{\rho}''_i\bar{\mu}'_i,\ \bar{\rho}'_{Bi}\bar{\mu}''_{Bi} = \bar{\rho}''_{Bi}\bar{\mu}'_{Bi}\ (i = K, T) \quad \text{(A8)}$$

required by "microscopic reversibility," as well as of the result that the binding constants of the internal site are the same for both bound and unbound pores:

$$\frac{\bar{\rho}'_i}{\bar{\mu}''_i} = \frac{\bar{\rho}'_{Bi}}{\bar{\mu}''_{Bi}}\ (i = K, T) \quad \text{(A9)}$$

which follows from "microscopic reversibility" and assumption (6)

Appendix B

Zero-Current Conductance of a Two-Site, Three-Barrier Channel with Mixed-Ion Double Occupancy

From the diagram in Fig. 13 it is apparent that in the presence of two permeant cations, a two-internal-site pore with double occupancy in the mixed case only can exist in seven different states. For simplicity we shall only consider pores with energy profiles symmetric with respect to the central peak. The rate constants of translocation across such a peak will be denoted by λ' and λ'', while those for the lateral barriers will be denoted by the same letters as were used in the previous model. However, considering that double occupancy is allowed for, each of these constants will have two values, depending on whether the adjacent site is empty or occupied. Two suffixes will be used in the latter case. For example, the rate constant for entry of ion K^+ into the left site from the left solution will be denoted by ν'_K if the right site is empty and by ν''_K if occupied by Tl^+. For singly occupied channels the binding constants of either site are most naturally defined by

$$K_i = \frac{\bar{\rho}'_i}{\bar{\mu}''_i} = \frac{\bar{\rho}''_i}{\bar{\mu}'_i}\ (i = K, T). \quad \text{(B1)}$$

It is also convenient to introduce the binding constants K'_K and K''_T, defined as

$$K^j_i = \frac{\bar{\rho}^{ij'}_i}{\bar{\mu}^{ij''}_i} = \frac{\bar{\rho}^{ij''}_i}{\bar{\mu}^{ij'}_i}\ (i,j = K, T;\ i \neq j) \quad \text{(B2)}$$

which, through "microscopic reversibility" are related to the others by

$$K_i K_j^i = K_j K_i^j. \tag{B3}$$

From the diagram in Fig. 13 it is clear that the fluxes of K^+ and Tl^+ will be given by

$$\phi_K = \lambda_K' N_2 - \lambda_K'' N_3 \qquad \phi_T = \lambda_T' N_4 - \lambda_T'' N_5 \tag{B4}$$

where N_l indicates the number of channels (per unit area) in state l. The mean current per unit channel will be equal to the sum of the two fluxes multiplied by e/N^T, e being the unitary charge and N^T the total number of pores per unit surface. The steady-state values of the N_l's can be calculated, according to a standard procedure, by solving a system of kinetic equations in which the net variation in density of channels in each state is set equal to zero. For example, for N_2 we shall have

$$\frac{dN_2}{dt} = [\nu_K' N_1 - \mu_K'' N_2] + [\lambda_K'' N_3 - \lambda_K' N_2] + [\mu_T^{K'} N_6 - \nu_T^{K''} N_2] = 0. \tag{B5}$$

Of the seven homogenous equations of this type that can be written only six are independent. From any group of six of these equations and the equation of conservation of the total number of channels,

$$\sum_1^7 N_l = N^T \tag{B6}$$

the explicit values of each of the N's can be derived. Substituting in (B4) one can finally obtain explicit expressions for the fluxes, the current density and the conductance. The final result for the zero-current conductance can be written

$$g_0 = g_{K0} + g_{T0} \tag{B7}$$

where

$$g_{K0} = \frac{2 g_K^{\max} K_K C_K}{1 + 2[K_T C_T + K_K C_K (1 + K_T^K C_T)]} \cdot \left\{ \frac{1 + \frac{\omega}{\bar{\mu}_K'} \left(1 + \frac{2\bar{\lambda}_T'}{2\bar{\lambda}_T' + \bar{\mu}_T'}\right) K_T^K C_T \left(1 + \omega \frac{K_K^T C_K}{\bar{\mu}_T' + 2\bar{\rho}_T'}\right)^{-1}}{\frac{\omega}{\bar{\mu}_K'} \left(\frac{\bar{\mu}_K'}{2\bar{\rho}_K' + \bar{\mu}_K'}\right) K_T^K C_T \left(1 + \omega \frac{K_K^T C_K}{\bar{\mu}_T' + 2\bar{\rho}_T'}\right)^{-1}} \right\} \tag{B8}$$

and g_{T0} is obtained from Eq. (B8) by interchanging K and T in all indices. In Eq. (B8) $g_K^{\max}$ and ω are defined as

$$g_K^{\max} = \frac{e^2}{kT} \frac{2\bar{\lambda}_K' \bar{\mu}_K'}{2\bar{\lambda}_K' + \bar{\mu}_K'}; \quad \omega = \frac{\bar{\mu}_K^{T'} \bar{\mu}_T^{K'}}{\bar{\mu}_K^{T'} + \bar{\mu}_T^{K'}}. \tag{B9}$$

Note that ω is symmetrical with respect to the indices K and T, and that $g_T^{\max}$ is obtained from $g_K^{\max}$ by replacing K with T. The two parameters in Eqs. (B8) which cannot be deduced from measurements in single salt are ω and K_T^K (K_K^T is related to K_T^K by the relation (B3) where K_K and K_T are determined from experiments in single-salt solutions).